Evaluation of Dynamic Response of an Asphaltic Concrete Core Rockfill Dam Using Newmark Approach (a case study)

A. Akhtarpour
Maharab Consulting Engineers Co.,Mashhad, Iran.

A. Khodaii
Department of Civil and Environmental Engineering, Amirkabir University of Technology, Tehran, Iran.

A. Ebrahimi & A. Zohourian
Maharab Consulting Engineers Co.,Mashhad, Iran.

ABSTRACT: Equivalent Linear Dynamic analyses have been performed for the highest dam with asphalt concrete core in Iran (Shur River dam) under seismic forces. The dam has 85 meters height and is under construction in an area with high earthquake hazard with MDE equal to 0.8 g. Different stages of construction and impounding were analyzed using the elasto-plastic model with Finite Element Method. Newmark approach utilizing the software Quake/W and Slope/W from Geostudio 2007 package were used to investigate asphaltic core behavior under earthquake loading. It is concluded that deformations along a predefined failure surface is composed of a circular arc that terminates at the upstream embankment crest. Estimated deformation with Slope/W using the Newmark method could have a value in excess of 2.0 m so that earthquake shock can lead to developing some cracks and increasing permeability of asphalt in the upper part of the core. Furthermore under sever shaking; shearing off of the thin core near the crest may occur.

1 INTRODUCTION

Asphaltic concrete has been used for 50 years as an impervious interior core curtain in hydraulic structures such as embankment dams (Hoeg, 1993, ICOLD,1992). Monitoring these dams has indicated their good behavior and performance during construction and operation for many years (Hoeg, 1993, ICOLD,1992,). However, most of the dams have been constructed in regions with low or moderate earthquake hazard and there is not any publications on actual dam behavior under sever earthquakes, so behavior of the dams in high seismic hazard areas needs more attention and exploration. In this study, the data from Shur dam with a height of 85 *m* (Highest ACRD dam in Iran) which is under construction was selected as a study case. The results from numerical analyses will show the response of this kind of core under static and dynamic loading.

2 SHUR RIVER DAM

Shur dam that is under construction in south of Kerman province, is the highest asphaltic rockfill dam in Iran. It has a height of 85 meters and is located in a U shaped long valley. The crest length of the dam is about 450 m and the vertical asphaltic concrete core, has 1.2 m width at the bottom decreasing to 0.6 m on the top, and is surrounded by filters (zones 2a) and transitions in upstream and downstream (zones 2b). The seismicity of the region is very high with MDE equal to 0.8g (ATC, 2008). Typical cross section of the Shur dam is shown in figure 1.

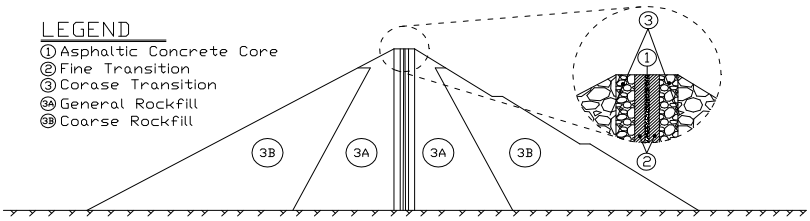

Figure 1. Typical cross section of the Shur dam.

3 NEWMARK APPROACH UTILIZING THE GEOSTUDIO 2007 SOFTWARE

3.1 *Overview*

A seismic deformation analysis of the embankment was conducted using the software programs Quake/W and Slope/W. Initial Pseudo static seismic analysis showed that upstream slope is more critical than downstream slope so the analysis was undertaken on the upstream embankment slope only. Quake/W and Slope/W was utilized to calculate the internal stresses and the estimated factor of safety of the embankment against failure along a critical failure surface as a function of time. The software then applies the Newmark Approach to estimate the degree of permanent deformation along the critical failure surface as a function of time.

3.2 *Geometry conditions*

The simplified embankment model and the finite element mesh (FEM) used in analysis is shown in Figure 2.

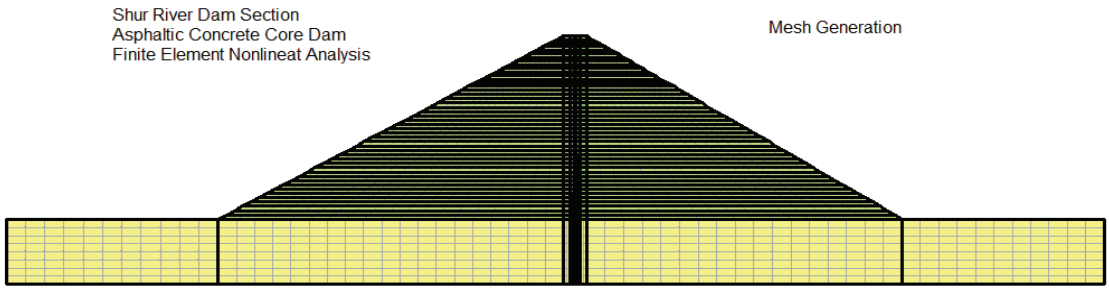

Figure2. Finite Element Mesh Generation.

Based upon the elastic properties of the materials used for the dam, the compression and shear wave speeds are (ATC, 2008):

Cp = 753 m/sec

Cs = 413 m/sec

For accurate representation of wave transmission in the model, during dynamic analyses, the spatial element sizes were selected small enough to satisfy the following criteria expressed by Kuhlemeyer and Lysmer (1973):

$$\Delta l \leq \frac{\lambda}{10} \tag{1}$$

Where λ is the wave length associated with the highest frequency component that contains appreciable energy and l is the length of the element.

4 STATIC ANALYSIS

Static analyses were carried out for various stages. The elasto-plastic Mohr-coulomb model was used. Table 1 presents the material properties used for numerical analyses. Effective E-modulus of the rock fill considered to be a function of effective stress as shown in Figure 3.

Table 1.Embankment Material Mohr-Coulomb Properties (ATC, 2008).

Material	γ (Kg/m3)	E (MPa)	υ	C (kN/m^2)	φ	Ψ
Asphalt	2420	150	0.49	360	18	0
Rockfill	2200	Fig.3	0.23	0	47	10
Transition	2150	18	0.3	0	38	8

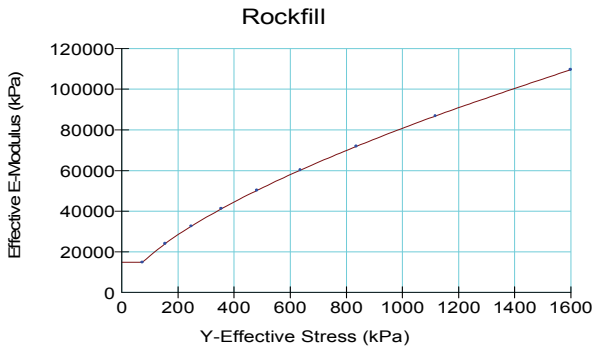

Figure3. Effective E-Modulus of rockfill as a function of effective stress.

4.1 *End of construction stage*

The analyses were performed using staged construction in 45 layers. Figure 4 shows the vertical displacements contours. The maximum settlement occurs inside the shell. The amount of maximum settlement is nearly 0.58 m. Figure 5 shows effective vertical stresses.

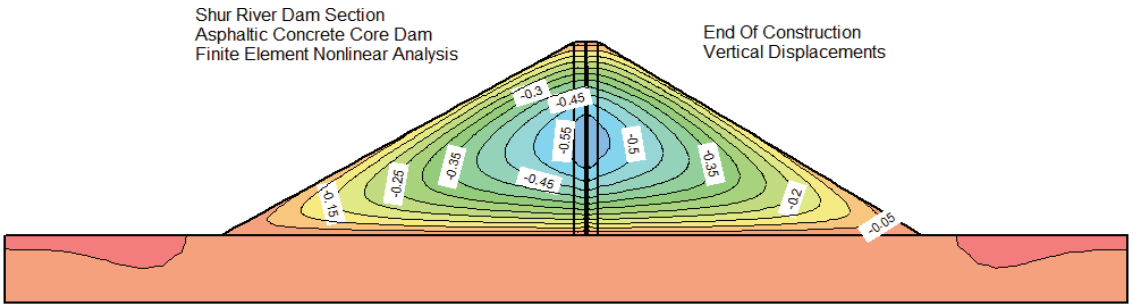

Figure 4. Vertical displacements contours at the end of construction stage (m).

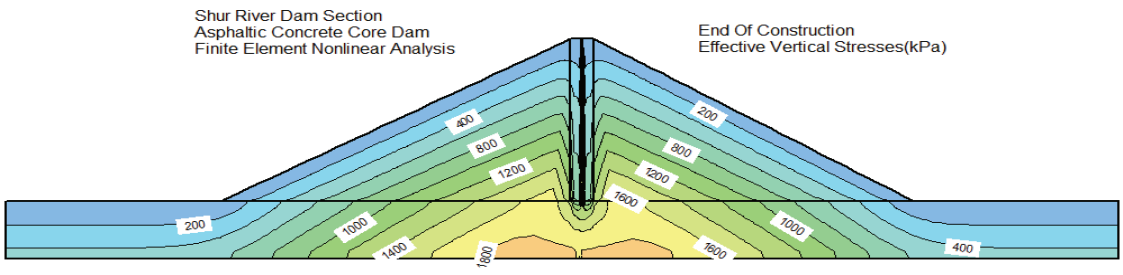

Figure 5. Effective vertical stresses contours at the end of construction stage (kPa).

4.2 *Impounding stage*

Water level increases to a height of 80 *m* above the base at three stages. During impounding, the hydrostatic force acts on the surface of the asphalt core because permeability of asphalt concrete in comparison with the shell and transition materials is very low. The adopted permeability coefficients for different materials are presented in Table 2.

Table 2. Embankment material hydraulic properties.

Material	Bedrock	AsphaltCore	Zones 2a/2b	Zone 3
Permeability (m/s)	$1x10^{-6}$	$1x10^{-11}$	$1x10^{-4}$	$1x10^{-2}$

A flow analysis has been carried out for modeling each stage of impounding following a stress redistribution phase to adjust effective stresses and pore pressures.
Figure 6 shows the predicted pore pressure contours after first filling to full supply level. The pattern of the pore pressure contours appears to be reasonable.

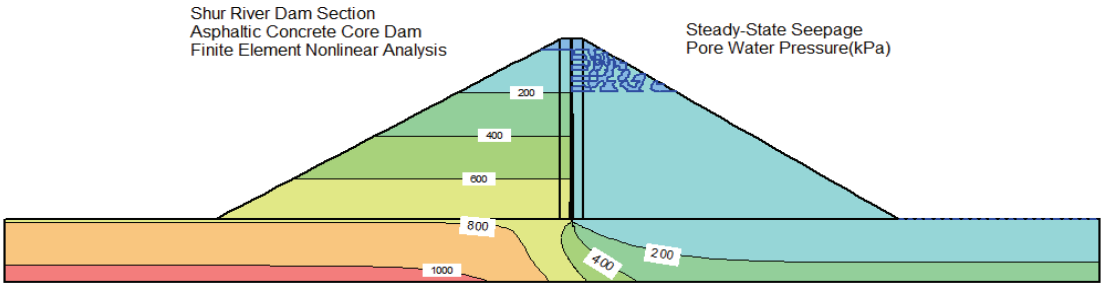

Figure 6. Pore pressure contours after impounding (kPa).

5 DYNAMIC ANALYSIS

5.1 *Input ground motion*

ATC consulting engineers co. (2008) in their seismicity report on the Sarcheshmeh site has proposed three alternative ground motion records suitable for seismic analyses.

From the two horizontal components of the acceleration-time histories the most severe component was used for the modeling. All waves were normalized to MDE acceleration.

As can be seen in Figure 7, most of the energy in the input motions are at frequencies less than 15, 15 and 20 Hz for Loma Prieta, Cape Mendocino and Nahanni earthquakes respectively.

The seismic records were filtered to remove frequencies greater than the above frequencies. The filtering process was performed to limit the size of elements and to ensure accurate wave transmission.

After filtering was completed, the waves were corrected for a base line drift (i.e. continuing residual displacement after the motion has finished).Finally the input motion to the model was applied as an acceleration time history to the base of the model. Standard earthquake boundary conditions suggested by the software manual (Geostudio, 2007) has been used for the analysis.

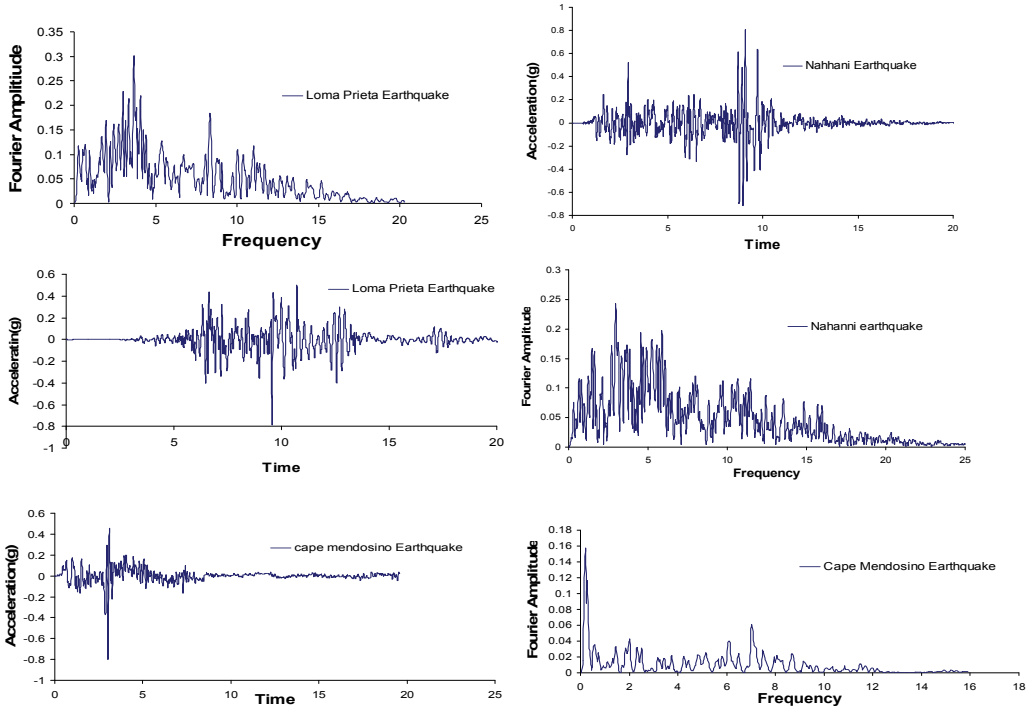

Figure 7. Time history and frequency domain for Nahanni, Loma Prieta and Cape Mendocino earthquakes.

5.2 *Material properties*

Stiffness and damping properties of the embankment materials used in the FEM analysis are summarized in Table 3, and are discussed in the following sections.

Table 3. Stiffness and damping properties of embankment material.

Material	Poison's Ratio	Shear Modulus G (MPa)	Initial Damping (%)	Modulus Reduction & Damping Curve
Bedrock	0.23	2,700	1	Schnabel (1973)
Asphalt Core	0.49	2500	1	Nakamura(2004)
Zone 2	0.3	*19.8 $\sigma_m^{0.5}$	1	Ishibashi (1993)
Zone 3	0.23	*37.4 $\sigma_m^{0.5}$	1	Ishibashi (1993)

* σ_m is the mean effective stress

5.2.1 *Rockfill friction angle*

K. J. Douglas (2002) after analyzing a large database of test results developed Equation (2) for shear strength of rockfills:

$$\sigma'_1 = RFI.\sigma'^{\alpha}_3 \tag{2}$$

The best estimation for α is 0.8726 and RFI is a multiplier depending on initial porosity, angularity, maximum particle size, percent of fines and unconfined compressive strength.
For the Shur dam Rockfill with regards to mean confining stresses at the base of sliding circles and rockfill properties, the best estimation is 47°.

5.2.2 *Shear modulus*

The small strain shear modulus, G_{max}, was determined using the methods described by Kramer (1996) and the seismic refraction test results of the main dam foundation area (ATC, 2008). G_{max} for the bedrock was calculated using the average shear wave velocity of 1050 m/s (measured in seismic refraction tests).

For Zone 2 and Zone 3, the G_{max} values were determined using the empirical relationship developed by Seed & Idriss (1984) as follows:

$$G_{\max} = 220 K_{2\max} . \sigma_m^{0.5} \quad (3)$$

Where K_{2max} is the shear modulus coefficient and a function of relative density and soil types. For a good quality rockfill (i.e. Zone 3), K_{2max} ranges from 120 at the surface to 180 at a depths of 100 m. A value of 170 was adopted for Zone 3 rockfill. For the transition zones (Zone 2) a value of 90 was adopted (Seed, 1970). Figure 8 shows G_{max} function and variation in shear modulus with cyclic shear strains.

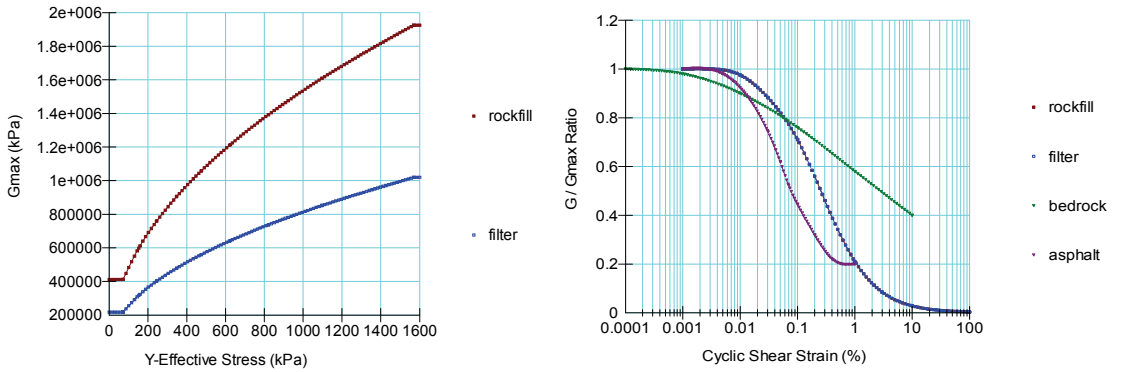

Figure 8. Variation in shear modulus curves for zone 2&3 (Ishibashi, 1993), bedrock (Schnabel, 1973) and asphalt (Nakamura, 2004).

5.2.3 *Damping*

The adopted curves for bedrock are from Schnabel (1973) , and the curves for Zone 2 and Zone 3 are from Ishibashi (1993). These curves were applied to the materials in the numerical model. The Adopted Curves for Asphaltic Concrete are from Nakamura (2004) using curve fitting method. Figure 9 illustrates assumed curves for asphaltic core, rockfill, filter and bedrock.

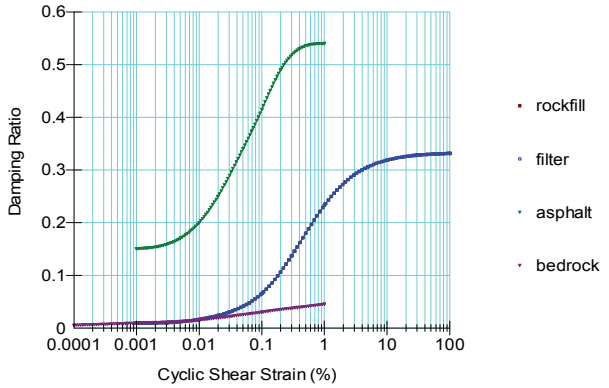

Figure 9. Variation in damping curves for zone 2&3 , bedrock and asphalt (Nakamura,2004).

6 SUMMARY OF ANALYSIS OF RESULTS

6.1 *Crest acceleration and displacements*

Crest acceleration and horizontal displacements as a function of time are shown in Figure 10 for the Lomaprieta earthquake as an example.

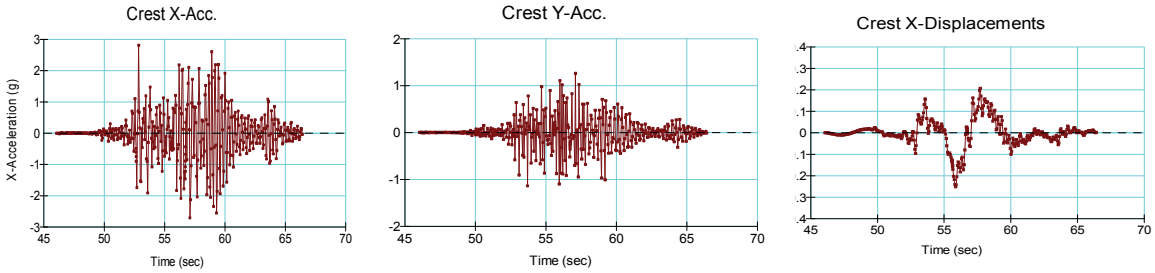

Figure 10. Crest horizontal and vertical acceleration and horizontal displacements as a function of time for Loma Prieta earthquake.

The predicted peak crest acceleration varies between 1.3 g to 3.0 g as compared to the input peak acceleration of 0.8 g implying an amplification of 1.6 to 3.7. These ranges of amplifications are expected for rockfill embankment dams based on past experience reported in many studies (Baziar, 2006, Feizi,2004, Ghanooni,2002) . Past studies by authors using Finite difference nonlinear method show less crest accelerations (ranges between 1.1 g to 1.8 g) (Akhtarpour,2010). This is in agreement with previous experiments that showed, generally equivalent linear method results more crest accelerations than fully nonlinear method in embankment dams (Feizi, 2004, Ghanooni,2002).

6.2 *Deformation analysis using Newmark approach*

The Slope/W deformation analysis was undertaken in consideration of two specific failure surfaces, firstly a circular arc terminating in the upper quarter of the upstream embankment face, secondly a circular arc terminating at the upstream embankment toe. For this analysis, cohesion of the asphalt core was ignored and an effective angle of friction of $\Phi = 40$ degree was adopted. If a crack developed in the asphalt core as a result of shear strains, embrittlement, or other unknown effects, this assumption could be considered to be true. As an example the figures 11 and 12 show the results of the toe and crest circles. (loma Prieta earthquake). The failure surface with the minimum factor of safety for the period of seismic motion analyzed is shown.

The total deformation calculated for both these failure modes are summarized in Table 4.

Table 4. Summary of predicted deformation from Newmark approach.

Earthquake	Predicted Peak Crest Acceleration (g)		Predicted Crest Settlement (m)	
	Horizontal	Vertical	Crest Failure Circle	Toe Failure Circle
Loma Prieta	2.8	1.26	2.25	0.94
Nahanni	3.0	2.0	1.68	0.65
Cape Mendocino	1.3	0.74	0.83	0.2

Also shown in Figure 13 is permanent deformation along the failure surface terminating in the upper quarter of the upstream embankment face, factor of safety and average acceleration as a functions of time for the Loma Prieta earthquake.

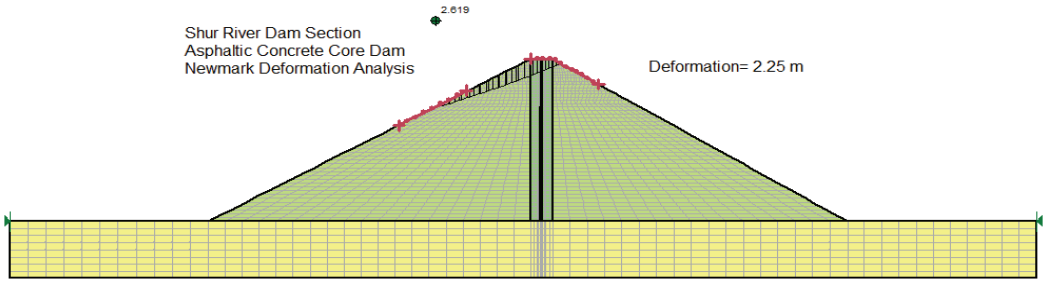

Figure 11. Crest failure surface related to maximum deformation for Loma Prieta earthquake.

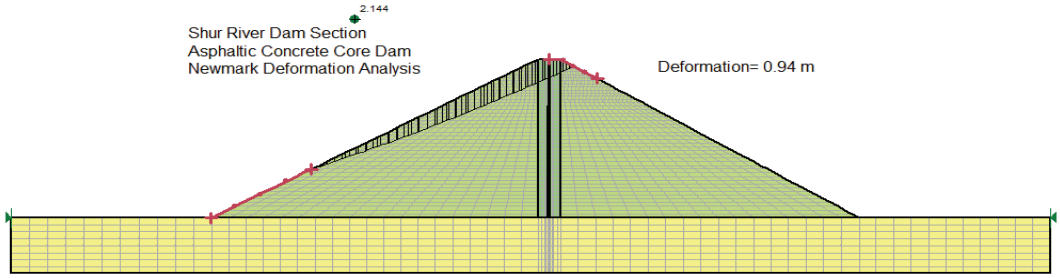

Figure 12. Toe failure surface related to maximum deformation for Loma Prieta earthquake.

It is concluded that deformations along a predefined crest failure surface, could be considered to have a value in excess of 2.25 m. The maximum crest settlement resulted from the Loma Prieta ground motion record with a vertical displacement of 2.25 m (Figure 13).

The magnitude of the estimated deformations appears to be large but does not exceed the embankment freeboard of 4.0 m.

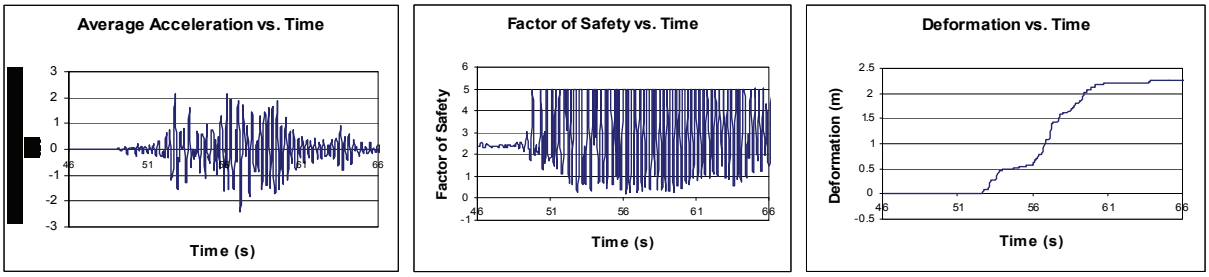

Figure 13. Average acceleration, factor of safety and deformation vs. time for crest failure surface from Loma Prieta earthquake.

In these method, it is conservatively assumed that the permanent shear displacements are all concentrated along a single shear surface through the core. In reality the shear distortion may be distributed vertically over a shear zone and thus be less likely to open a gap between the top and lower part of the impervious core. Past studies by authors using fully nonlinear FDM method resulted upstream crest deformation equal to 2.15, 1.71 and 1.01 meter for each of ground motion records respectively that are in a good agreement with this study (Akhtarpour, 2010).

7 SUMMARY AND CONCLUTIONS

- The maximum predicted deformation of the rockfill is a vertical deformation of 2.25 m, determined using the Newmark approach. Under normal operating conditions a minimum freeboard of 4.0 m is provided between crest level and spillway level, thus, deformations of this magnitude would not cause the storage to be breached and are considered to be acceptable
- During an extreme earthquake, the induced permanent displacements for an embankment dam may become so large that a narrow core is sheared off and a gap opens. Then it will be the depth of the gap beneath the water level and the permeability of the filter/transition zones that will govern the magnitude of the leakage rate until the reservoir water level is lowered.
- For such an eventuality it would be advisable to have a relatively fine-grained material next to the asphaltic core. In any case, it is essential that the downstream shell and toe is designed with adequate drainage capacity to handle accidental leakage and prevent dam failure even if the temporary water loss is dramatic.
- The results of the analysis indicate that the maximum deformations will occur near the crest and at the upper part of the upstream slope.
- At the levels of permanent deformations observed, plastic deformation of the core is expected, and cracking of the core and increasing permeability may occur in the upper 15 meter of the dam. At this level water pressure is not enough to cause leakage and failure.
- Based on the numerical analysis using Newmark approach, all critical sliding surfaces cross from above 70 m height of the dam, hence it seems that reduction in core thickness with the height of the dam, as considered in design, is not appropriated.

REFERENCES

Akhtarpour Ali, Khodaii Ali, (2010) "Nonlinear Numerical evaluation of Dynamic behavior of an Asphaltic Concrete Core Rockfill dam (a Case study)", JSEE Journal, Fall 2009, Vol. 11, No. 3

Australian Tailing Cosultants, ATC, (2008) Design report, Shur river dam,

Baziar,M.H., Salemi,Sh., Heidari,Ta.,(2006),"Analysis of earthquake response of an Asphalt Concrete Core Embankment Dam", Int. Journal. Of Civil Eng. (IUST), Vol.4, No.3, September 2006

Douglas kurt John, (2002) "The Shear Strength of Rock Masses", Ph.D. Thesis, School of Civil and Environmental Eng, Sydney Australia, Chapter 4, December 2002.

Feizi-Khankandi, S., Mirghasemi, A.. A., Ghanooni, S.(2004). "Behavior of Asphaltic Concrete Core Rockfill Dams", Published in International conference on Geotechnical Engineering(ICGE) (UAE)

Geo-Slope International, Ltd. Geostudio (2007) user manual, Calgary, Alberta, Canada, 1991-2008

Ghanooni, S. and Mahin Roosta, R.(2002),"Seismic analysis and design of asphaltic concrete coredams," Journal of Hydropower and Dams, 9, Issue 6, 75-78,.

Hoeg, K.. (1993). Asphaltic Concrete Cores for Embankment Dams, Norwegian Geotechnical Institute of Technology, Oslo,(Norway)

ICOLD Press, Bituminous cores for earth and rockfill dams, Bulletin 42& 84, 1982, 1992

Ishibashi,I. and Zhang,X.J.(1993),"Unified dynamic shear module and damping ratios of sand and clay", Soils and Foundations,Vol.33,No.1,pp.182-191.

Kuhlemeyer, R.L. and Lysmer, J. (1973)., Finite element method accuracy for wave propagation problems, J. of soil mechanics and foundations, Div. ASCE, 99(SM5), 421-427

Kramer, Steven, Jan (1996). Geotechnical earthquake engineering, Prentic-Hall International Series in Civil Engineering Mechanics,(USA)

Nakamura, Y., Okumura, T., Narita, K. and Ohne, (2004) Y., "Improvement of impervious asphalt mixture for high ductility against earthquake excitation," Proc. New Developments in Dam Engineering, 647-656,.

Schnabel,P.B.(1973). Effects of Local Geology and Distance from Source on Erthquake Ground Motions,Ph.D. Thesis, University of California,Berkeley,California.

Seed, H.B., Idriss, I.M. (1970) "Soil module and damping factors for dynamic response analyses", Report EERC 70-10, Earthquake Engineering Research Centre, University of California, Berkeley.

Seed, H.B. , Wong, R.T. , Idriss, I.M., (1984),"Module and damping factors for dynamic analyses of cohesion-less soils, Journal of geotechnical engineering,Vol.112,No.11,pp. 1016-1032.